www.czasopisma.pan.pl PAN POLSKA AKADEMIA NAUK www.journals.pan.pl

Arch. Metall. Mater. **64** (2019), 4, 1533-1540

DOI: 10.24425/amm.2019.130123

A. BRZEZIŃSKA*#, A. URBAŃCZYK-GUCWA*, R. MOLAK**, K. RODAK*

MICROSTRUCTURAL FEATURES AND MECHANICAL PROPERTIES AFTER APPLYING ROLLING WITH CYCLIC MOVEMENT OF ROLLS OF AN Al-Li ALLOYS

Two strength-age hardening aluminum-lithium alloys: Al-2.3wt%Li and Al-2.2wt%Li-0.1wt%Zr in two different heat treatment conditions: solution state (S) and additionally in aging state (A) were severely plastically deformed by rolling with cyclic movement of rolls (RCMR) method to produce ultrafine – grained structure. Two thermo-mechanical treatments were used: (S+A+RCMR) and (S+RCMR+A+RCMR). To investigate the combined effect of plastic deformation and heat treatment, tensile tests were performed. Microstructural observations were undertaken using scanning transmission electron microscopy (STEM), and scanning transmission electron microscopy (SEM) equipped with electron backscattering diffraction detector (EBSD). Based on the obtained results, it can be deduced that maximum mechanical properties as: yield strength (YS) and ultimate tensile strength (UTS) could be achieved when the microstructure of alloys is in (S+A+RCMR) state. For samples in (S+RCMR+A+RCMR) state, ductility is higher than for (S+A+RCMR) state. The microstructural results shows that the favourable conditions for decreasing grain size of alloys is (S+A+RCMR) state. Additionally, in this state is much greater dislocation density than for (S+RCMR+A+RCMR) state. The microstructure of alloys in (S+RCMR+A+RCMR) state is characterized by grains/subgrains with higher average diameter and with higher misorientation angles compared with (S+A+RCMR) state.

Keywords: Al-Li alloy, severe plastic deformation, ultrafine-grains, STEM, SEM/EBSD

1. Introduction

Severe plastic deformation (SPD) allow to generate nano- and ultrafine grained microstructures in order to produce high strength combined with suitable ductility in metals and alloys. Traditional Al alloys very frequently are deformed in the solution heat treated conditions especially due to increase the workability during deformation [1-4]. Generally, microstructure refinement of Al, and especially Al alloys by SPD processing have received much interests for their potential in significant increase of mechanical properties [5-8].

Al-Li alloys, which belong to 8xxx series are commonly used as a material for aerospace applications [9,10] because exhibit a good combination of low density, high elastic modulus and high strength [11,12]. The attractive properties of Al alloys and also Al-Li alloys are associated with the presence of alloying elements which enable formation of strengthening precipitates [13-16]. The major problem in these alloys is tendency for strain localization. The negative effect of this phenomenon is formation of macroscopically visible on the surface deformation bands, which can initiate crack and failure of the sample [17,18]. Obviously, SPD processing in room temperature of Al-Li alloy can leads to formation of shear band. From literature is known that the δ' phase, which is a metastable, coherent and have a spherical morphology is known to provide strengthening, but also to cause strain localization and decrease ductility [9,18]. Precipitation hardening process allows formation equilibrium phases and strain localization should be suppressed. Additionally thanks to precipitation hardening effect, the high strength is obtained. Although ultrafine-grained (UFG) Al-Li alloys have high mechanical properties in comparison with their coarse-grained (CG) counterparts, their ductility (uniform ductility)are rather low [3]. The develop structural materials with simultaneous high strength and ductility it has been an important goal for Al-Li alloys because these alloys have an interesting physical and mechanical properties.

In the present study, was proposed SPD deformation process in combination with solid solution strengthening and precipitation strengthening for Al-Li (Al-2.3wt%Li and Al-2.2wt%Li-0.1wt%Zr) alloys was proposed. Combined process of heat treatment and deformation performed by using rolling with cyclic movement of rolls (RCMR) method [19,20] has been proposed in order to improve ductility of mentioned alloy. RCMR has been widely used for alloys based on aluminium and copper [21,22]. The present work is focused on the microstructure and mechanical properties investigations of Al-Li alloys after applying thermo-mechanical treatments.

* SILESIAN UNIVERSITY OF TECHNOLOGY, FACULTY OF MATERIALS ENGINEERING AND METALLURGY, 8 KRASIŃSKIEGO STR., 40-019 KATOWICE, POLAND
** WARSAW UNIVERSITY OF TECHNOLOGY, FACULTY OF MATERIALS ENGINEERING, 141 WOŁOSKA STR., 02-507 WARSZAWA, POLAND
# Corresponding author: agata.brzezinska@polsl.pl

2. Experimental

The Al-2.3wt%Li and Al-2.2wt%Li-0.1wt%Zr alloys were applied for the investigations. In the present work, the following heat treatment processes are used: solution treatment followed by quenching into iced water at 500°C for 1h (S), aging treatment followed at 200°C for 12h (A). The processing conditions chosen for microstructure and mechanical properties investigations were the next:

1) state 1: (S+A+RCMR),
2) state 2: (S+RCMR+A+RCMR).

In this experiment, RCMR process was realized at the total effective strain $\varepsilon_{ft} = 5$ with the following parameters: rolling rate $v = 1$ rpm, amplitude of transverse movement of rolls $A = 0.8$ mm, frequency of transverse movement of rolls $f = 2$ Hz.

The total effective strain ε_{ft} was expressed as:

$$\varepsilon_{ft} = \sum_{i=1}^{n} \sqrt{\varepsilon_{hi}^2 + \varepsilon_{ti}^2} \tag{1}$$

$$\varepsilon_{hi} = \ln \frac{h_i}{h_{i-1}} \tag{2}$$

$$\varepsilon_{ti} = \frac{4fA\sqrt{(h_{i-1} - h_i)\frac{D}{2}}}{\sqrt{3}v(h_{i-1} + h_i)} \tag{3}$$

where: ε_{ft} – total effective strain, ε_{hi} – strain included by rolling reduction, ε_{ti} – strain included by transverse movement of working rolls, n – number of passes, h_{i-1}, h_i – height of sample before and after unit pass (reduction), A – amplitude of cyclic movement, f – frequency of rolls movement, D – diameter of the rolls (here 100 mm), v – rolling rate.

The rolling reduction (absolute reduction of the height of the sample after RCMR deformation) $\varepsilon_h = 80\%$ (initial height –8 mm, height after deformation ~1.6 mm). For S+A+RCMR state, the process was realized into 5 passes. For S+RCMR+A+RCMR state, the number of passes was 5. Aging process was performed after 3 passes.

Scanning transmission electron microscopy (STEM) was carried out in a Hitachi HD-2300A microscope operated at 200 kV. Thin foils for (STEM) were prepared by electropolishing using (TENUPOL 5) device manufactured by Struers, Inc. Electron backscattering diffraction (EBSD) was conducted in a FEI INSPECT F field emission gun- scanning electron microscope (FEG-SEM) equipped with a EBSD detector and TSL OIM software. Specimens were polished by using an ion thinning device (PECS) manufactured by Gatan, Inc.

In this work, microstructural investigations and mechanical properties evaluated by tensile testing were carried out for microareas where, the effect of grain refinement was evident. For this reason, the microstructural investigations were made in the transverse plane section in the distance about ~0.8 height of the specimens. More information's presented in [22].

The FEG-SEM observations were made in the transverse plane section in the distance about 0.8 height of specimens. STEM analysis was not possible on transverse section due to small dimensions of the sample. For this reason, STEM observations of the thin foils parallel to the rolling plane were performed from a distance of 0.8 height of specimens. The tensile tests were conducted at room temperature at the constant initial strain rate of 2×10^{-3} s^{-1}. Due to the limited amount of the material available for testing, and heterogeneity of deformation [22] microtensile samples with total length and thickness of 8.6 mm and 0.3 mm, respectively, were used to evaluate the mechanical properties. The samples were produced by wire-cut electro-discharge machining (W-EDM) parallel to the rolling plane direction. The mechanical properties were determined using an MST Qtest/10 machine equipped with digital image correlation (DIC) [23,24]. Four tensile tests were performed on each sample and the average values and standard deviations were calculated.

3. Results

The microstructure of alloys consist of almost equiaxial grains with dimension about ~300 mm. During aging treatment form precipitates as shown in Fig. 1.

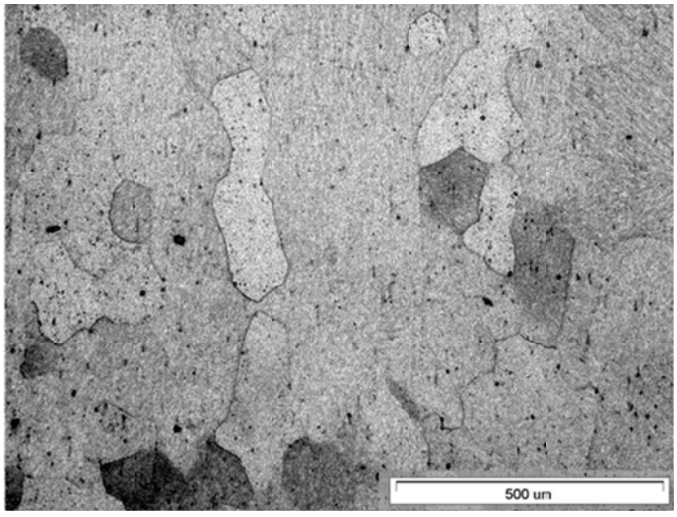

Fig. 1. Microstructure of Al-2.3wt%Li-0.1wt%Zr alloy in aging state

As a results of aging (A), strengthening precipitates of δ' (Al_3Li) phase in Al-2.3wt%Li and additionally β' (Al_3Zr) phase in Al-2.2wt%Li-0.1wt%Zr are formed [25,26]. Carefully inspection of the precipitates reveals that the morphology of the precipitates seems to be spherical. The size of the precipitates in both alloys are in range of 20-50 nm. The precipitates are quite homogeneously distributed in the matrix Fig. 2.

RCMR deformation result in the formation of characteristic shear bands with a width of approximately one micron (Fig. 3). Inside shear bands the fine-grained microstructures are shown.

Alloys were examined by EBSD in the transverse section and the results are presented in Figs. 4, 5 and in Table 1. In the EBSD maps, the thin lines represent the boundaries having smaller misorientation θ in the range of $2° \le \theta < 15°$, while the

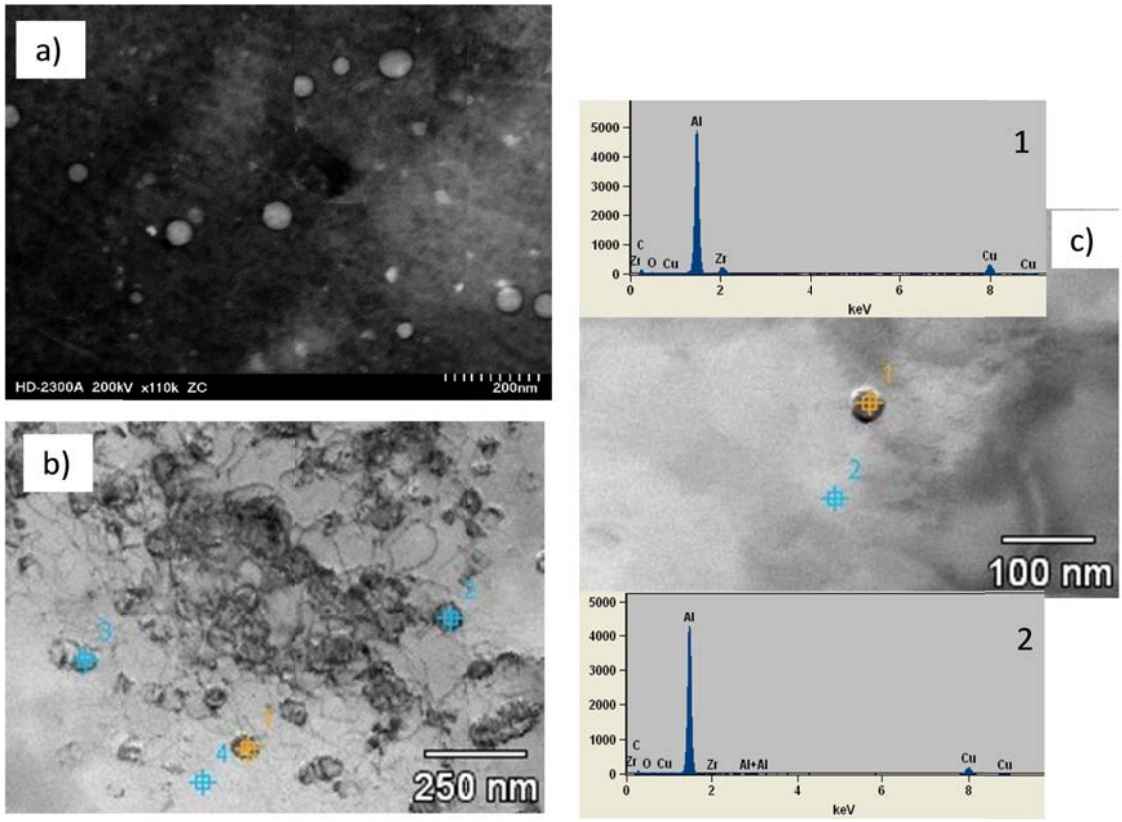

Fig. 2a-c). Al_3Zr precipitates in Al-2.3wt%Li0.1wt%Zr alloy obtained for S+A+RCMR state. a) dark field, b) bright field, c) EDS spectrum from marked points

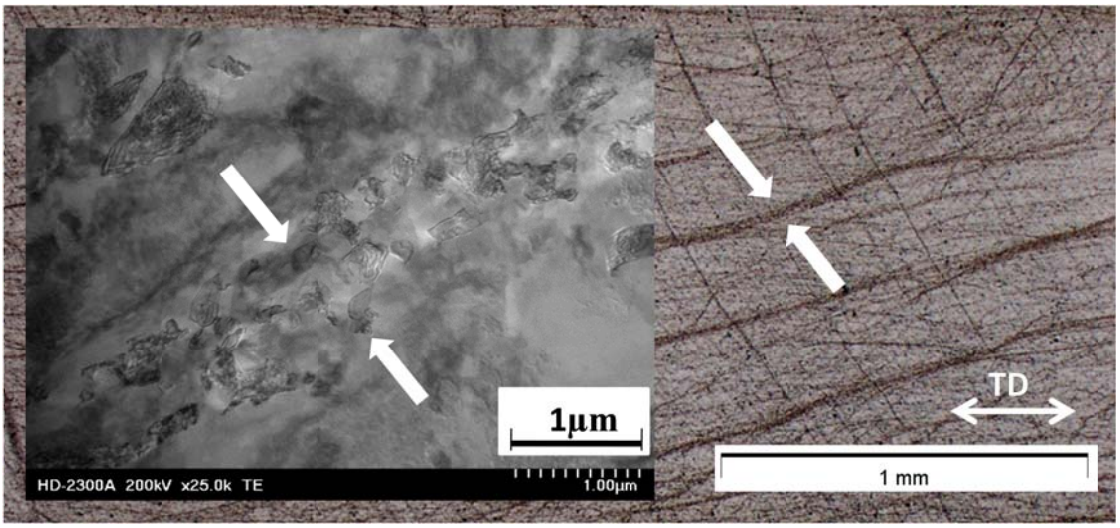

Fig. 3. Shear bands in Al-2.3wt%Li alloy. S+A+RCMR state

bold lines represent the boundaries with larger misorientation of $15° \leq \theta$. Low angle boundaries with misorientation smaller than 2° were out of consideration. The strong influence of the processing conditions on the microstructure formation was evident.

On EBSD maps (Figs. 4,5) it is difficult to see a grain/subgrain completely enclosed by boundaries, for this reason it may be complicated for interpretation. This situation may be the results of high dislocation density in grain boundaries. It was evident that, the grain boundaries have mixed character, with high and low angles of misorientation independently of the chemical composition of analyzed alloys. Although, the microstructure of (S+RCMR+A+RCMR) state is characterized by grains/subgrains with higher misorientation angles compared with (S+A+RCMR) state (Figs. 4a, 5a, Table 1). For example the fraction of high angle boundaries (HABs) in Al-2.3wt%Li-0.1wt%Zr alloy is 7% for (S+A+RCMR) state and 28% for (S+RCMR+A+RCMR) state. Generation of high fraction of high angle boundaries HABs observed for state (S+RCMR+A+RCMR) state is additionally

connected with creation of more granular grains. On EBSD maps are well visible ultrafine equiaxed grains with random orientation and the location of the new grains is not accidental. These new grains are mainly associated with shear bands. Presence of shear bands visible in particularly for (S+A+RCMR) state influence on inhomogeneous distribution of grain size in (S+RCMR+A+RCMR) state. Especially it was visible for Al-2.3wt%Li-0.1wt%Zr alloy (Fig. 5b). Based on EBSD investigations it worth nothing that the obtained grain/subgrain sizes for Al-2.3wt%Li and Al-2.2wt%Li-0.1wt%Zr alloys in (S+A+RCMR) state are smaller than grain/subgrain obtained for (S+RCMR+A+RCMR) state (Table 1). For example the grain size of Al-2.3wt%Li alloy is about 220 nm for (S+A+RCMR) state and ~420 nm for (S+RCMR+A+RCMR) state. Similar results in grain measurement were obtained for Al-2.2wt%Li-0.1wt%Zr alloy ~260 nm and ~410 nm for (S+A+RCMR) and (S+RCMR+A+RCMR) (Table 1). The obtained results shows that the favourable conditions for decreasing grain size is (S+A+RCMR) state. Generally, the EBSD investigations exhibited that processing for (S+RCMR+A+RCMR) state results in increase of grain/subgrain size and increase of average misorientation of boundaries.

Fig. 6 shows STEM analysis of RCMR processed of Al-2.3wt%Li and Al-2.3wt%Li-0.1wt%Zr alloys for (S+RCMR+A+RCMR) state. Microstructural characterization with using STEM method for (S+A+RCMR) state is presented elsewhere [22]. The obtained results with using STEM shows that S+RCMR+A+RCMR process leads to recovery by formation of equiaxed structure. For Al-2.3wt%Li alloy has been developed a structure of new equiaxed grains/subgrains with dislocations inside or without dislocations, with sharp boundaries (Fig. 6a,b). Most of the grains are separated by high angle boundaries. Additionally are visible wavy boundaries with high energy and in non-equilibrium state. These results are confirmed by EBSD measurement, where sum of medium angle boundaries (MABs) and HABs exceeds of 50%. The precipitates observed in grain boundaries and inside grains are able to pin dislocation and boundary migration (Fig. 6a,b). In the microstructure of

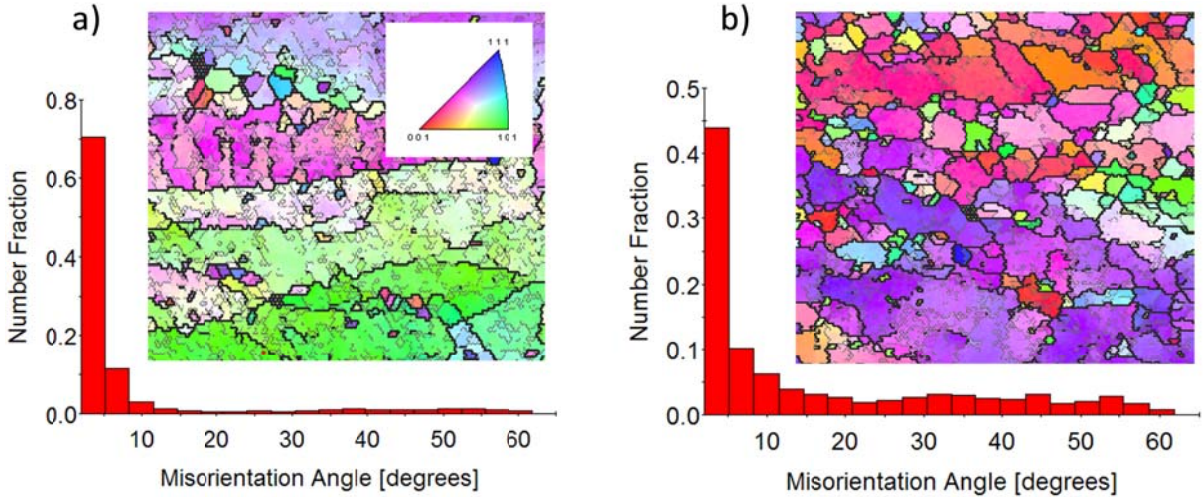

Fig. 4. Boundary maps of Al-2.3wt%Li alloys obtained by using STEM/EBSD method. Black lines mark boundaries with misorientation >15° (HABs), while gray lines mark oundaries with misorientation between 2° and 15° (LABs): a) S+A+RCMR state, b) S+RCMR+A+RCMR state

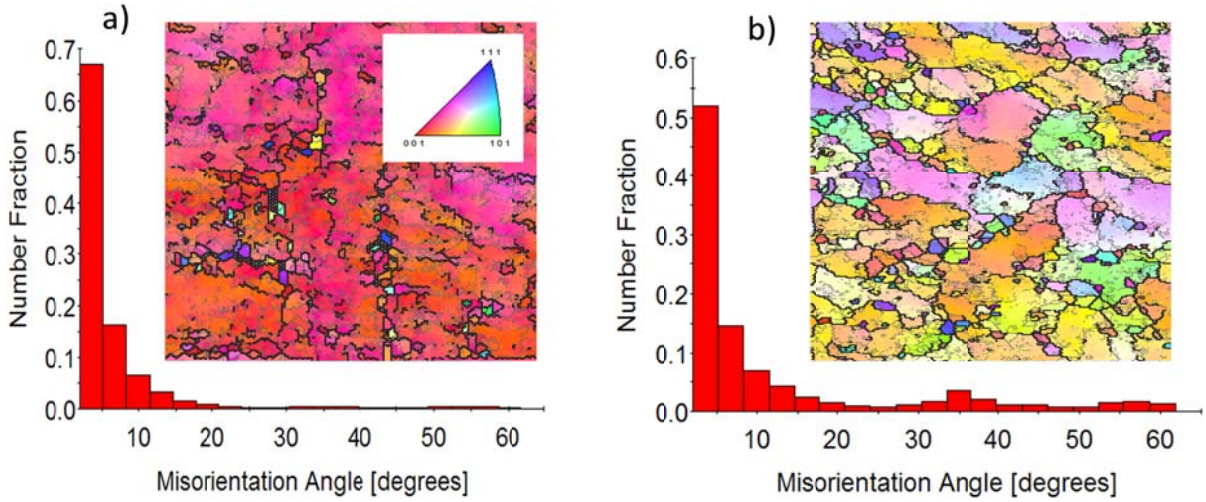

Fig. 5. Boundary maps of Al-2.3wt%Li-0.1wt%Zr alloys obtained by using STEM/EBSD method. Black lines mark boundaries with misorientation >15° (HABs), while gray lines mark oundaries with misorientation between 2° and 15° (LABs): a) S+A+RCMR state, b) S+RCMR+A+RCMR state

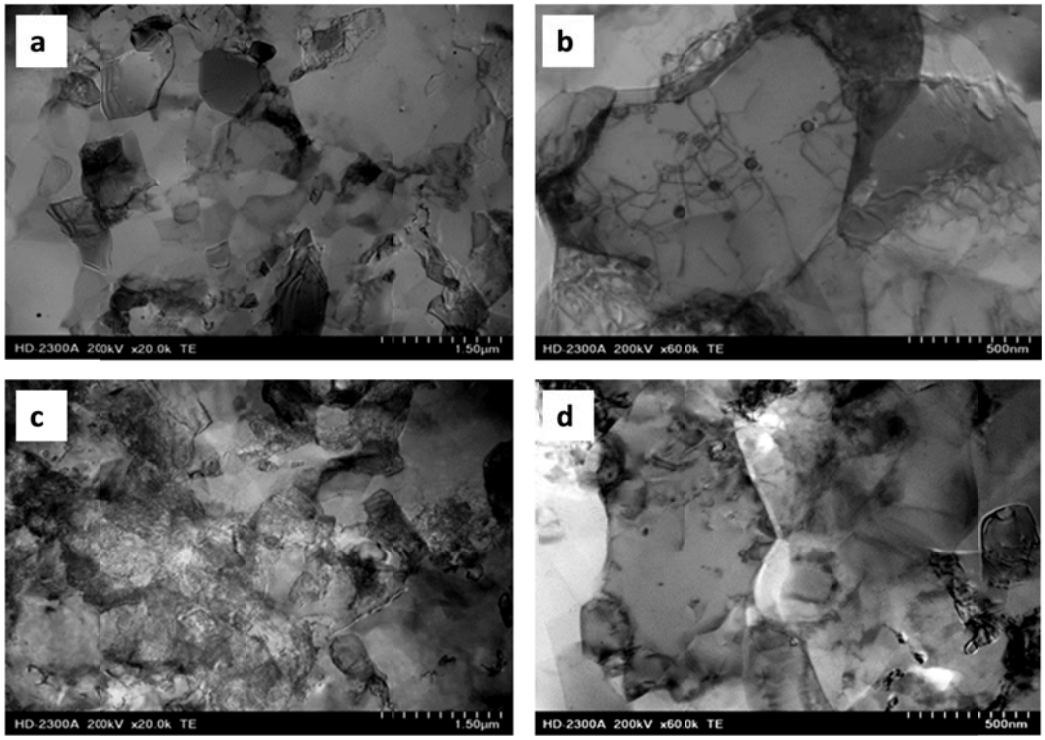

Fig. 6. Scanning transmission electron microscopy (STEM) bright field images of S+RCMR+A+RCMR state obtained for: a,b) Al-2.3wt%Li alloy, c,d) Al-2.3wt%Li0.1wt%Zr alloy

Al-2.3wt%Li-0.1wt%Zr alloy are visible grains/subgrains with high dislocation density. More dislocations are pinned by the precipitates (Fig. 6c,d). Additionally many of grain/subgrain boundaries are ill-defined. Nonetheless, many of the grains are separated by HABs. Although the sum of medium MABs and HABs exceeds only of 50%.

TABLE 1

Measured microstructural parameters: subgrain/grain size obtained by STEM measurements (d/D_STEM), average misorientation ($\theta_{Avg.}$), fraction of high angle boundaries (HABs), fraction of medium angle boundaries (MABs) of Al-Li alloys deformed with RCMR processing

	Material state	d/D (nm) STEM	θ Avg. (°)	HABs >15° (%)	MABs 5°-15° (%)
Al-2.3wt%Li	S+A+RCMR	222±3	8.9	13	17
	S+RCMR+A+RCMR	420±11	16	36	21
2.2wt%Li-0.1wt%Zr	S+A+RCMR	257±7	6.5	7	28
	S+RCMR+A+RCMR	410±17	12	28	28

In the samples after RCMR are observed a strong increase in yield stress (YS) and ultimate tensile stress (UTS) with significant decrease in uniform elongation (A_{gt}) and elongation to fracture (A_c) compared to material in initial state (Table 2). The microstructures obtained for discussed states have evident influence on the mechanical properties. Figs. 7, 8 and Table 2 shows the true stress vs. true strain of the processed alloys. Processing conditions of alloys in (S+A+RCMR) state results in a strong increase of strength properties compared with (S+RCMR+A+RCMR) state. For example, for (S+A+RCMR) state and (S+RCMR+A+RCMR) state of Al-2.2wt%Li alloy the (YS) was about 302 MPa and 167 MPa respectively. Samples of Al-2.2wt%Li-0.1wt%Zr alloy attained higher (YS) and (UTS) compared with samples of Al-2.2wt%Li alloy for comparable processing conditions (Table 2). The alloys after RCMR deformation shows elongation to fracture (A_c) in the range (0.4%-4%). Uniform elongation (A_{gt}) obtained for deformed alloys were in the range (0.4%-1.6%). Uniform elongation (A_{gt}) is more than two times higher for (S+RCMR+A+RCMR) state in both alloys than in (S+A+RCMR) state. For example, for (S+A+RCMR) state and (S+RCMR+A+RCMR) state of Al-2.2wt%Li-0.1wt%Zr alloy the (A_{gt}) was about 0.48% and 1.6% respectively.

TABLE 2

Measured mechanical parameters: yield strength (YS), ultimate tensile strength (UTS), uniform elongation (A_{gt}), elongation to fracture (A_c) of deformed Al-Li alloys with RCMR processing

	Material state	YS (MPa)	UTS (MPa)	A_{gt} (%)	A_c (%)
Al-2.3wt%Li	initial state	39±6	90±8	41.0±0.5	53.0±1
	S+A+RCMR	302±8	303±6	0.4±0.3	0.4±1
	S+RCMR+A+RCMR	167±5	178±6	1.1±0.2	2.0±0.6
2.2wt%Li-0.1wt%Zr	initial state	88±5	141±9	14.9±0.5	47.0±0.7
	S+A+RCMR	309±11	313±14	0.48±0.9	0.64±0.6
	S+RCMR+A+RCMR	194±13	234±15	1.6±0.8	4.0±1

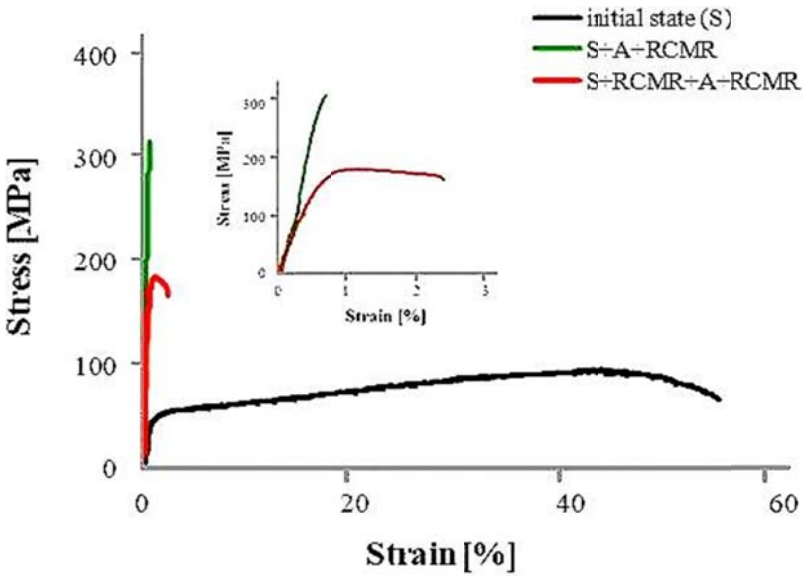

Fig. 7. Engineering stress-strain curves of Al-2.3wt%Li alloy

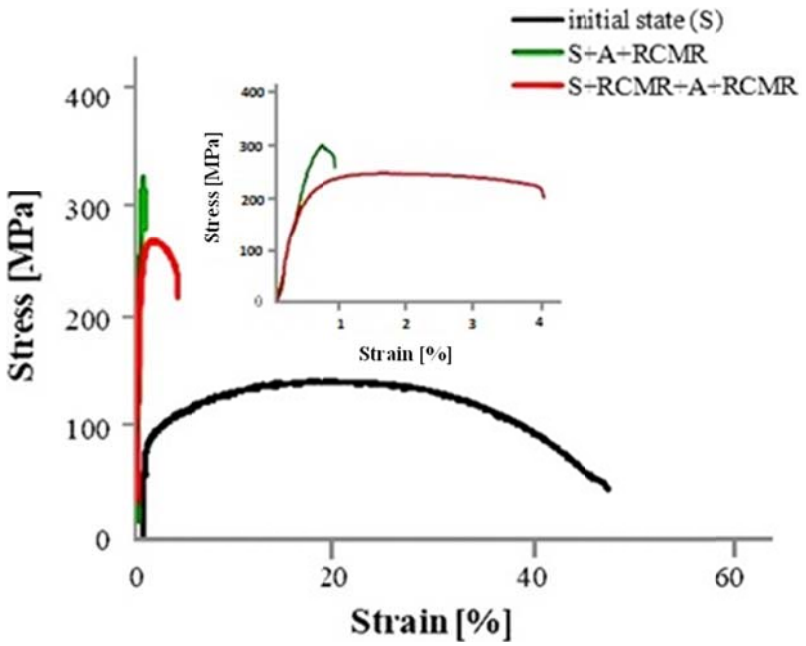

Fig. 8. Engineering stress-strain curves of Al-2.2wt%Li-0.1wt%Zr alloy

4. Discussion

The results exhibited that the strength properties as YS and UTS for (S+A+RCMR) state are higher than that of the (S+RCMR+A+RCMR) state (Table 2). It is evident from obtained results, that there is a clear dependence between the obtained grain/subgrain size (Table 1) and YS, where the YS increase with decrease of grain/subgrain size. The obtained results shows that available conditions for decreasing the grain size is presence in alloys of second phase particles. However, as it was demonstrated the conditions of thermo-mechanical treatment, which allow secondary phase produce, influence on grain refinement during RCMR. As a results of aging (A), strengthening precipitates of δ' (Al_3Li) phase in Al-2.3wt%Li and additionally β' (Al_3Zr) in Al-2.2wt%Li-0.1wt%Zr alloy were observed with the dimensions about 20-50 nm (Fig. 2). From literature it is known, that addition of Zr to aluminium alloys processed by SPD can lead to reduction of recovery rate during deformation and inhibit recrystallization and abnormal grain growth [25,26]. Additionally, coherent Al_3Zr precipitates can pin moving dislocations and grain boundaries and shift recrystallization to higher temperatures [27]. However, the strengthening effect of δ' (Al_3Li) and β' (Al_3Zr) decreases with the increasing of particle diameter at elevated annealing temperature [27,28]. In your investigations, with using STEM it was obtained that precipitates of Al_3Zr especially at (S+A+RCMR) state for both alloy reduces the mobility of dislocation, which leads to much more denser dislocations distributions [22]. The samples

exhibit a subgrain/grain with high dislocation density interior and with low angle boundaries in predominately compared with (S+RCMR+A+RCMR) state.

The results exhibited that the strength properties depend on chemical composition (Table 2). It was evident, that greater amount of secondary particles in Al-2.2wt%Li-0.1wt%Zr alloy results in increase of dislocation density in deformed matrix (Fig. 6). The experimental results indicate that the high strength may be achieved by the strengthening from dislocation.

The EBSD maps obtained from (S+RCMR+A+RCMR) state shows that the structure is characterized by considerable creation of equiaxial grains with higher misorientation angles compared with (S+A+RCMR) state (Figs. 4,5). Dislocation structure is more heterogeneously in the alloy of (S+A+RCMR) state. Especially characteristic features for (S+A+RCMR) state as mentioned previously is much greater dislocation density [22] than in (S+RCMR+A+RCMR) state. This gives the evidence that dynamic recovery mechanism has the meaning in (S+RCMR+A+RCMR) state. Dislocations are rearrangement, annihilated and are also absorbed to the grain boundaries. Such a rebuilding of a dislocation structure during aging process after deformation results facilitate the increase of grain boundaries misorientation (Figs. 4b,5b). Re-deformation of alloys after aging especially influence on increase of dislocation density (Fig. 6). Obtained during aging precipitates can increase the rate of dislocation generation by formation of Orovan loops [9,29].

The results of mechanical properties indicate that processed samples especially for (S+RCMR+A+RCMR) state may possess an enhanced uniform elongation (A_{gt}) and elongation to failure (A_c) (Table 2). In these state the microstructures consist of well-defined grains/subgrains with the low dislocation density inside the grains/subgrains and with high fraction of medium and high-angle boundaries compared with samples for (S+A+RCMR) state. According to the literature, the improvement in the ductility can be achieved due to an increasing number of HABs and the presence of fine dislocation-free grains with different orientations [30], this features of microstructure (Fig. 4,5, Table 1) are privileged to increase of ductility (Fig. 7,8). Additionally, it is visible another feature of microstructures in S+RCMR+A+RCMR state, namely bimodal grain-size distribution. Especially it is visible in Fig. 5b. From literature is known that introducing a bimodal grain-size distribution has been demonstrated an efficient strategy for obtaining high-strength and ductile metallic materials, where fine grains provide strength, while coarse grains enable strain hardening and hence decent ductility [31].

Bimodal grain size distribution is a consequence generation of shear bands during RCMR deformation. This type of inhomogeneous plastic flow involving very large local strains, occurs in a variety of material after SPD deformation [32]. According with literature it is known that this phenomenon is especially observed during cyclic deformation tests after changing strain path [33,34]. The presence of numerous microshear bands may be the characteristic feature of the deformation structure in the aging state, where coherent precipitates are observed. It is very likely that high local stress concentrations due to the high dislocation density exceeded the critical stress of shear band formation. In many materials inside shear bands dislocation tangles are observed [35]. In your experiment are observed shear bands with a very fine equiaxed highly disoriented grains. Researched alloys belong to materials with high stacking fault energy (SFE). In materials with high SFE the dynamic recovery time was very short, therefore, the transition from the dislocation tangle to the high- angle grain boundaries does not require more energy [34,36]. For this results fine grains are observed inside shear bands. Generally, in this experiment (S+RCMR+A+RCMR) state offers increase in ductility but simultaneously is not able to cause an increase in YS and UTS.

5. Summary

In this article the effect of thermomechanical treatment conditions on the microstructure and mechanical properties of Al-Li alloys were investigated. Applied thermo-mechanical processing results in formation of δ' (Al_3Li) and β' (Al_3Zr) precipitations. Particles has a very strong effect on structure refinement by inhibiting recovery and occurring the less dynamic boundary migration. During RCMR deformation the grain boundaries and dislocations were strongly pinned by fine precipitates. Conditions of thermo-mechanical treatment influence on grain refinement during RCMR. The S+A+RCMR process results in the formation of structure, where regions with fine-grained structure as well as regions with less refinement structure can be observed. Applied S+RCMR+A+RCMR process intensifies the formation of subgrain structure, and grain refinement process because increase number of fine-grained regions. Most of the grain boundaries have high angles boundaries. For S+RCMR+A+RCMR state increase of average grain/subgrain size and decrease dislocation density. The grain refinement on the mechanical properties was determined on the basis of tensile test on the micro samples. The S+RCMR+A+RCMR process leads to an decrease of strength and increase of ductility compared with S+A+RCMR process. Grain refinement and dislocations are responsible for the strengthening effect of alloys. Obtained results indicate existence in the RCMR deformed structure of shear bands.

REFERENCES

[1] N.V. Isaev, P.A. Zabrodin, V.Z. Spuskanyuk, A.A. Davydenko, V.V. Pustovalov, V.S. Fomenko, I.S. Braude, Low Temp. Phys. (2012). DOI: 10.1063/1.3678178

[2] S. Kobayashi, T. Yoshimura, S. Tsurekawa, T. Watanabe, J. Cui, Mater. Trans. **44**, 1469-1479 (2003). DOI: 10.2320/matertrans.44.1469

[3] K. Wawer, M. Lewandowska, K.J. Kurzydlowskp, Arch. Metall. Mater. **57**, 877-881 (2012). DOI: 10.2478/V10172-0I2-0097-1

[4] E.K. Cardoso, V. Guido, G. Silva, W.B. Filho, A. Jorge, Rev. Mater. (2010).

[5] M. Vaseghi, A.K. Taheri, H.S. Kim, in: IOP Conf. Ser. Mater. Sci. Eng., 2014. DOI: 10.1088/1757-899X/63/1/012089

[6] K. Rodak, J. Pawlicki, M. Tkocz, Solid State Phenom. **191**, 37-44 (2012). DOI: 10.4028/www.scientific.net/SSP.191.37

[7] K. Rodak, K. Radwański, R.M. Molak, Solid State Phenom. (2011). DOI: 10.4028/www.scientific.net/SSP.176.21

[8] S. Fritsch, M.F. Wagner, Metals (Basel). **8**, 63 (2018). DOI: 10.3390/met8010063

[9] N. Jiang, X. Gao, Z.Q. Zheng, Trans. Nonferrous Met. Soc. China (English Ed. (2010). DOI: 10.1016/S1003-6326(09)60207-7

[10] M. Tan, T. Sheppard, M. Tan, T.S. Extrusion, P. Of, A.N.A. Alloy, (1987).

[11] B. Adamczyk-Cieślak, J. Mizera, K.J. Kurzydłowski, Mater. Sci. Eng. A (2010). DOI: 10.1016/j.msea.2010.04.032

[12] G.J. Kulkarni, D. Banerjee, T.R. Ramachandran, Bull. Mater. Sci. (1989). DOI: 10.1007/BF02747140

[13] M.H. Shaeri, M.T. Salehi, S.H. Seyyedein, M.R. Abutalebi, J.K. Park, Mater. Des. (2014). DOI: 10.1016/j.matdes.2014.01.008

[14] P.J. Apps, M. Berta, P.B. Prangnell, Acta Mater. (2005). DOI: 10.1016/j.actamat.2004.09.042

[15] O. Novitović, Ž. Kamberović, A. Novitović, Metalurgija (2010).

[16] B.B. Straumal, B. Baretzky, A.A. Mazilkin, F. Phillipp, O.A. Kogtenkova, M.N. Volkov, R.Z. Valiev, Acta Mater. (2004). DOI: 10.1016/j.actamat.2004.06.006

[17] Y.B. Xu, W.L. Zhong, Y.J. Chen, L.T. Shen, Q. Liu, Y.L. Bai, M.A. Meyers, Mater. Sci. Eng. A (2001). DOI: 10.1016/S0921-5093(00)01412-X

[18] M. Furukawa, A. Utsunomiya, K. Matsubara, Z. Horita, T.G. Langdon, Acta Mater. (2001). DOI: 10.1016/S1359-6454(01)00262-2

[19] Z. Cyganek, K. Rodak, F. Grosman, Arch. Civ. Mech. Eng. **13**, 7-13 (2013). DOI: 10.1016/J.ACME.2012.10.008

[20] Patent no. PL 203220 B1, b.d.

[21] K. Rodak, A. Urbańczyk-Gucwa, M.B. Jabłońska, Arch. Civ. Mech. Eng. **18**, 500-507 (2018). DOI: 10.1016/j.acme.2017.07.001

[22] K. Rodak, A. Urbańczyk-Gucwa, M. Jabłońska, J. Pawlicki, J. Mizera, Arch. Civ. Mech. Eng. **18**, (2018). DOI: 10.1016/j.acme.2017.06.007

[23] R.M. Molak, H. Araki, M. Watanabe, H. Katanoda, N. Ohno, S. Kuroda, in: J. Therm. Spray Technol., 2014. DOI: 10.1007/s11666-013-0024-7

[24] R.M. Molak, M. Kartal, Z. Pakiela, W. Manaj, M. Turski, S. Hiller, S. Gungor, L. Edwards, K.J. Kurzydlowski, Appl. Mech. Mater. (2007). DOI: 10.4028/www.scientific.net/AMM.7-8.187

[25] A. Medjahed, H. Moula, A. Zegaoui, M. Derradji, A. Henniche, R. Wu, L. Hou, J. Zhang, M. Zhang, Mater. Sci. Eng. A **732**, 129-137 (2018). DOI: 10.1016/j.msea.2018.06.074

[26] H. Chen, T. Yu, Z. Qi, R. Wu, G. Wang, X. Lv, F. Cong, L. Hou, J. Zhang, M. Zhang, J. Mater. Eng. Perform. **27**, 5709-5717 (2018). DOI: 10.1007/s11665-018-3678-y

[27] H. Huang, F. Jiang, J. Zhou, L. Wei, J. Qu, L. Liu, J. Mater. Eng. Perform. (2015). DOI: 10.1007/s11665-015-1748-y

[28] Y. Wang, Z. Li, T. Yu, A. Medjahed, R. Wu, L. Hou, J. Zhang, X. Li, M. Zhang, Adv. Eng. Mater. **20**, 1700898 (2018). DOI: 10.1002/adem.201700898

[29] H. Jiang, S. Sandlöbes, G. Gottstein, S. Korte-Kerzel, J. Mater. Res. **32**, 4398-4410 (2017). DOI: 10.1557/jmr.2017.350

[30] S. V. Dobatkin, J. Gubicza, D. V. Shangina, N.R. Bochvar, N.Y. Tabachkova, Mater. Lett. **153**, 5-9 (2015). DOI: 10.1016/j.matlet.2015.03.144

[31] Y.M. Wang, E. Ma, Acta Mater. (2004). DOI: 10.1016/j.actamat.2003.12.022

[32] D. Sagapuram, K. Viswanathan, K.P. Trumble, S. Chandrasekar, Philos. Mag. **98**, 3267-3299 (2018). DOI: 10.1080/14786435.2018.1524586

[33] A. Korbel, W. Bochniak, Scr. Mater. **51**, 755-759 (2004). DOI: 10.1016/j.scriptamat.2004.06.020

[34] N.A. Sakharova, J.V. Fernandes, Mater. Chem. Phys. **98**, 44-50 (2006). DOI: 10.1016/j.matchemphys.2006.01.038

[35] D. Hughes, Mater. Sci. Eng. A **319-321**, 46-54 (2001). DOI: 10.1016/S0921-5093(01)01028-0

[36] T. Sakai, A. Belyakov, R. Kaibyshev, H. Miura, J.J. Jonas, Prog. Mater. Sci. **60**, 130-207 (2014). DOI: 10.1016/j.pmatsci.2013.09.002